*International Conference on Mechanical, Industrial and Energy Engineering 2022*
*22-24 December, 2022, Khulna, BANGLADESH*

ICMIEE22-003

# Condensate Characterization: An Approach to Evaluate the Performance of Condensate as a Feedstock in Oil Refinery

*Nadia Mahjabin*[1*], *Kakon Sultana*[1], *Dr. Md. Tazul Islam*[1], *Md. Mostafijul Karim*[1]
[1] Department of Petroleum and Mining Engineering, Chittagong University of Engineering & Technology, Chattogram-4349, BANGLADESH

**ABSTRACT**
During the distillation process, petroleum streams are created from crude oil, also known as petroleum fractions, which is a complex mixture of several hydrocarbon components. A refinery's technical design and process efficiency depend on the physical qualities of the feedstock, commonly known as assay information; however, a comprehensive compositional analysis of naturally occurring hydrocarbon mixtures is difficult and time-consuming. In order to produce assay data, based on both laboratory tests and computer-aided analysis, the goal of this work is to develop a method to a comprehensive and organized characterization of gas condensate as a refining feedstock. The study also focuses on a critical examination of the assay data from samples of gas condensate that were taken from Bangladesh's Rashidpur (RGF) and Kailashtila (KTL) gas fields. The study initially carried out laboratory tests to establish the boiling point and specific gravity. Empirical correlations are used to determine the necessary physical parameters for calculations involving the refining process. The actual boiling point (TBP) curve is constructed using the Riazi and Daubert model and Daubert's new approach, and the extrapolation of the Daubert curves results in the greatest recovery at the final distillation point. Then, utilizing Peng Robinson's thermodynamic model, DWSIM software helps create pseudo-components and their associated attributes using the generated TBP data. The results of this study demonstrated that combining lighter and heavier condensates efficiently can improve product quality and fuel performance of condensate, which can be used as a baseline to assess the performance of condensate as a refining feedstock.

Keywords: condensate; TBP distillation; physical parameter; pseudo-component; pseudo properties.

## 1. Introduction

The Petroleum stream constitutes a mixture of the complex hydrocarbon chain. Small petroleum cuts or pseudo-components generally characterize the streams, which are identified from the distillation curve [1,2]. Feedstock assay data are essential in the refining process because the assay provides an extensive and detailed analysis data of hydrocarbon [3].
As the rule of thumb, the high degree of fractionation gives detailed and accurate information on the component distribution. TBP curve (Figure 1), a graphical representation of the average boiling point of components against the volume percent of the distilled sample, has a smooth shape for a large number of components, and small distillation steps [4].

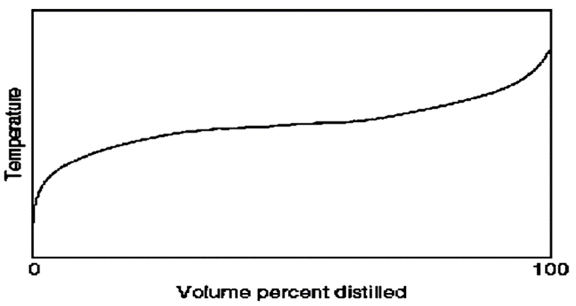


**Fig.1** Typical TBP curve of a petroleum mixture.

ASTM or TBP distillation curves show the volatile characteristics of petroleum streams. Although both are batch distillations, ASTM distillation requires a simple setup, takes less time, and is successfully automated. So, it is preferable to use ASTM to determine the distillation data, which are then converted into TBP data using empirical equations [5].
Natural-gas condensate is a mixture of low-boiling hydrocarbon liquid that is also referred to as condensate, gas condensate, or natural gasoline. Gas condensate at a refinery can be distinguished from distillate, a straw-colored liquid that is primarily made of naphtha [6]. Condensate is currently a major problem with both technical and financial repercussions [7]. Two condensate-rich gas fields in Bangladesh—the Rasidpur gas field (RGF) and the Kailashtila gas field—were used to acquire the condensate sample for this study (KTL). One of the oldest gas fields in Bangladesh is the gas condensate field known as Kailashtila [8]. With 5.2 TCF in reserve, the Rashidpur Gas Field is situated in Habiganj, Bangladesh [9]. Even though there have been numerous researchs on crude oil assay, this work is the first to attempt to produce condensate assay, compare two types of condensates from Bangladeshi gas fields, and assess the samples as a feedstock for refineries.
During the screening process, some research concluded that the current industrial standards for recognizing gas condensate reserves based on relative molecular weight are insufficient [10]. The API gravity thermodynamic property analysis can therefore be used to get over this limitation. This work generates the true boiling point curve, API curve, and specific gravity curve for the collected sample in order to characterize it. Second, DWSIM software is used to estimate the crucial properties. Additionally, it seeks to assess various prediction correlations in order to determine the final recovery at the final (100%) boiling point. In actuality, it is not possible to completely distillate an initial charge

* Corresponding author. Tel.: +88-01814354438
E-mail addresses: nadia.pme11@cuet.ac.bd

since the volatile components in the charge may remain after distillation and cannot be condensed again [10]. Here an investigation is done to generate a polynomial equation that can predict recovery at a 100% point. The work approaches to predict the physical properties of feed that can assist in qualifying the fractions or cuts in a refinery.

Condensate can be used as an alternate fuel source as our nation doesn't have many oil reserves and imports are the main supply of oil. In this study, several physical and thermodynamic properties are determined in an effort to determine how well condensate performs as a fuel. It provides a straightforward yet methodical method for determining which kind of condensate mixture would be more effective and practical to employ as an alternative fuel source.

## 2. Characterization of Petroleum Fraction

### 2.1 Defining Pseudo-Components

Pseudo components are the basis for characterizing the petroleum fraction in a refining process. The actual components, for example, paraffin, naphthenes, and aromatic, remain undetermined in fractionation; however, the process can detect a discrete number of mixtures point. The mixture corresponds to several unknown actual components, is termed a pseudo component, and has a defined cut point or boiling point range. One can treat the pseudo component as defined one as soon as the normal boiling point and specific gravity is determined [11].

### 2.2 ASTM D86 Test Method

In this process, the collected sample (usually 100 ml in amount) is distilled in a flask under specific conditions [11]. The flask is connected to an inclined condenser that condenses the rising vapors. A graduated cylinder collects the distilled fractions, and the temperature of the rising vapors is recorded at a specific interval of collected distillate. The initial boiling point (IBP) refers to the temperature at which the first drop of condensate is collected. When almost the entire sample is distilled (above 95%), the corresponding maximum temperature is called the endpoint (EP).

### 2.3 Conversion between ASTM and TBP Distillation

The TBP data gives detailed information on the volatile characteristics of crude oil or petroleum fractions.

#### 2.3.1 Riazi and Daubert/ API Method

Riazi and Daubert (1980) have developed a relation to performing the inter-conversion of the ASTM method and TBP distillation.

$$TBP = a(ASTM\ D86)^b \quad (1)$$

Here a and b are constants. TBP is calculated at a defined distillate point (like 0, 10, 30, 50, 70, 90, and 95 percent point), where the temperature is expressed in ˚R.

#### 2.3.2 Daubert Method

In 1994, Daubert proposed an updated method for inter-conversion based on the initial and final temperatures of distillation curves. The equations Eq. (2). suggested by Daubert are:

$$T'_{50}=A_4(T_{50})^{B4},\quad T'_{30}=T'_{50}-\Delta T'_3 \quad T'_{10}=T'_{30}-\Delta T'_2 \quad T'_0=T'_{10}-\Delta T'_1,$$
$$T'_{70}=T'_{50}+\Delta T'_5 \quad T'_{90}=T'_{70}+\Delta T'_6 \quad T'_{95}=T'_{90}+\Delta T'_7 \quad (2)$$

Where, $\Delta T'_i=A_i(\Delta T_i)^{B_i}$, $\Delta T_1=T_{10}-T_o$, $\Delta T_2=T_{30}-T_{10}$, $\Delta T_3=T_{50}-T_{30}$, $\Delta T_5=T_{70}-T_{50}$, $\Delta T_6=T_{90}-T_{70}$, $\Delta T_7=T_f-T_{90}$

The symbols T and T' stand for ASTM D86, and TBP temperatures, respectively, and are in ˚F. The subscripts 0 and f stand to represent the initial and final temperatures. $A_i$ and $B_i$ express the constants.

### 2.4 Generating Pseudo-components

The cuts in petroleum fraction have a specific boiling point range and specific properties like viscosity, API gravity. The number of cut points in a TBP curve determines the number of pseudo components, where a higher number of cut points help to reproduce the TBP curve accurately [4]. Although more components are required to produce a smooth property curve, a large number of components can delay the computation time. A general guideline has been suggested by considering these two facts [13].

## 3. Results and Analysis

### 3.1 Distillation Analysis

ASTM D86 distillation experiment in the laboratory gives the ASTM test data for both condensate samples (**Table 1**). Specific gravity is measured through ASTM D1298 test.

**Table 1** Distillation data for RGF & KTL

| Volume % | ASTM˚C (KTL) | ASTM˚C (RGF) |
|---|---|---|
| **0** | 48 | 48 |
| **10** | 84 | 84 |
| **30** | 100 | 100 |
| **50** | 114 | 114 |
| **70** | 136 | 136 |
| **90** | 210 | 210 |
| **95** | 259 | 259 |
| **EP.** | 310 | 273 |
| **Density @32(kg/L)** | 0.844 | 0.765 |

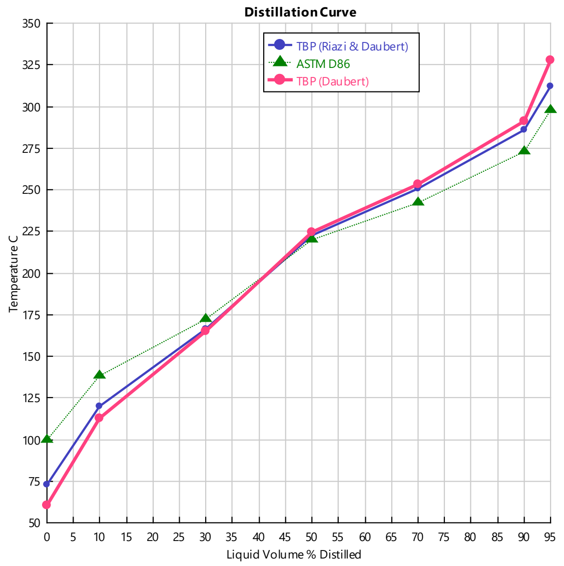


**Fig 2.** TBP curve for RGF condensate.

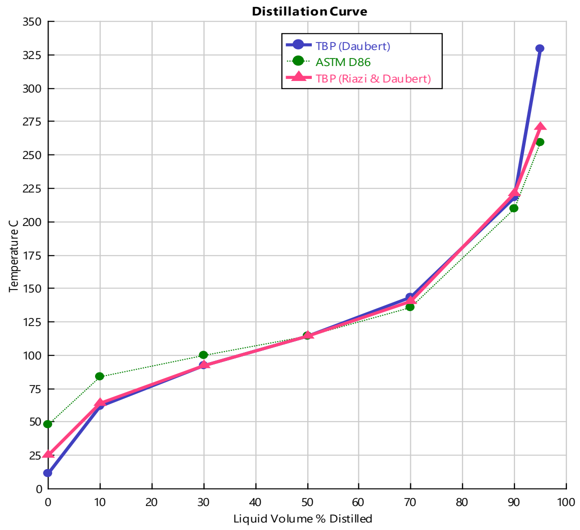


**Fig 3.** TBP curve for KTL condensate.

In this study, the ASTM data are transformed into TBP data using the Riazi/API method and Daubert correlation. The differences in the curves are seen in Figs. 2 and 3. The ultimate boiling point is greater than the real ASTM data in the figure, however the IBP is lower than the ASTM IBP point for both TBP procedures. Additionally, the final boiling point is substantially higher according to the Daubert estimate than it is according to the Riazi calculation. Because a TBP distillation test has a higher degree of separation than an ASTM distillation test, the findings are different. The EP for RGF ranges for a boiling range of 95% distillate. However, for KTL, the EP continues past the 95% point. Daubert's approach also has a substantially higher endpoint (EP) temperature for KTL condensate. This is due to the KTL's smaller weight and the presence of more volatile components at the curve's conclusion. The calculated findings of the physical characteristics of the condensate sample are tabulated in Table 2.

**Table 2** Calculated result of VABP, MeABP, MW, K & API gravity for KTL & RGF

| Field name | KTL | RGF |
|---|---|---|
| VABP | 263.84 | 408.272 |
| MeABP | 244.827 | 389.259 |
| K | 11.43882 | 11.07594 |
| SG | 0.778 | 0.855 |
| MW | 23.25854 | 37.86626 |
| API gravity | 50.37661 | 33.99708 |

The KTL condensate is lighter than the RGF condensate, which is further supported by calculations of average boiling temperatures and molecular weight. Additionally, as seen in Table 2, the heavier one has a significantly higher volume average boiling point.
The extrapolation of the curve to the final point (100%) is necessary to acquire the average boiling point of the last cut, which is needed to construct pseudo-components. This method bases the curve extrapolation on an Excel spreadsheet. The ASTM data are transformed into TBP data through relation. Fig 2

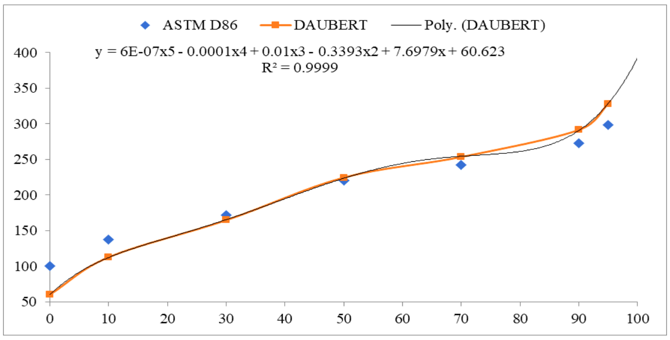


**Fig 4.** Extrapolation of Daubert TBP curve (RGF)

In order to determine the average boiling points of the final cuts, the Daubert's TBP curve is extrapolated in this article. According to Fig. 4, the curve fits a fifth-order polynomial function for the RGF sample. The correlation parameter's value is 0.99, indicating that the function and experimental findings have a fair degree of convergence.

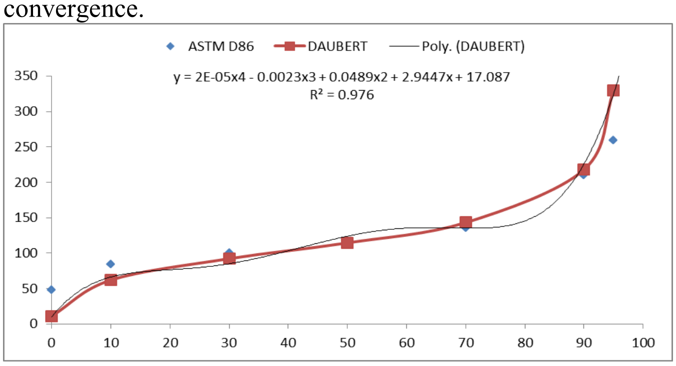


**Fig 5.** Extrapolation of Daubert TBP curve (KTL)

The extrapolation produces a fourth-order equation with a correlation parameter of 0.976 in the case of the KTL sample (Fig. 5). As a result, it displays a poor convergence with Daubert TBP data.

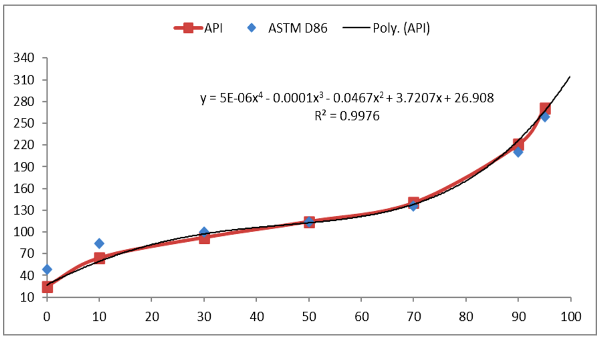


**Fig 6.** Extrapolation of API TBP curve (KTL)

On the other hand, when the API curve is extrapolated, the correlation parameter exhibits good convergence (R2 = 0.99). (Fig 6). For lighter condensate samples, it can therefore be claimed that the API curve is a preferable option for obtaining pseudo components. In order to compare the computed findings of heavier and lighter condensate in this study, a following calculation uses Daubert's TBP data.

### 3.2 Pseudo-components calculation

The pseudo-components on the RGF's TBP curve are identified in Fig. 7. According to general guidelines, the TBP curve is divided into 19 slices, and Daubert's TBP data shows that the boiling point range of RGF is between 60 and 400 C.

The cut range for RGF has been set as 60.45-364.39 C with a 15.99 C temperature interval. The first cut's EBP is IBP+15.99. The whole calculation process for the cuts, including whether the NBP is the average of the previous two EBP values, is shown in Appendix.

A lighter feed is KTL condensate. Here, the temperature intervals between each cut are 16.33 degrees Celsius, with temperature ranges between 11 and 340 degrees Celsius. The curve's EP is 337 °C. Daubert's TBP data extrapolated curve deviates little from the true TBP curve. However, the pseudo-component breakdown-generated TBP curve exhibits high symmetry with an ideal TBP curve. As a result, it can be concluded that Daubert's TBP data is a better option for figuring out the pseudo-component attributes.

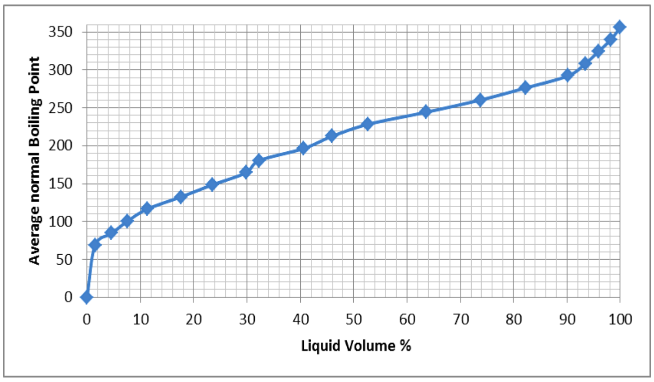


**Fig 7.** Representation of the TBP curve by pseudo-component (RGF)

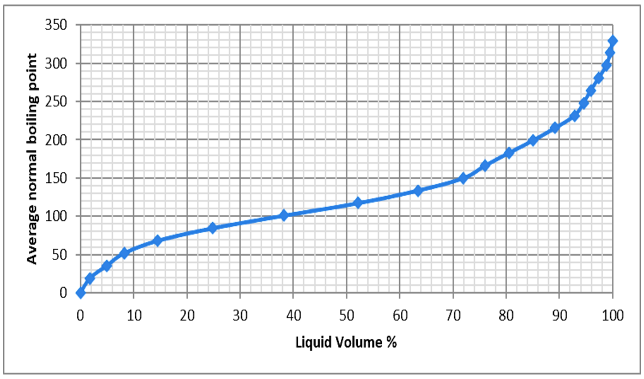


**Fig 8.** Representation of the TBP curve by pseudo-components (KTL)

#### 3.2.1 Parameter Determination

The study used the DWSIM software to produce fictitious components or cut points for comparison and validation. Cut points are determined using the Daubert's TBP data, specific gravity (SG), and molecular weight (MW) as input data. The components are by default named according on their mean average boiling points. The Riazi technique is used to calculate the SG, API gravity, and MW of each component, whereas Lee and Kessler's method is chosen to calculate the crucial characteristics, which serve as the input for calculating the thermodynamic properties. The aforementioned strategy is typically used by oil refineries.

The Watson characterisation factor (K) makes it possible to calculate gravity. A characteristic curve for a pseudo-component is the gravity versus NBP curve. The comprehensive outcomes of the simulation of crucial properties computation are displayed in the Appendix.

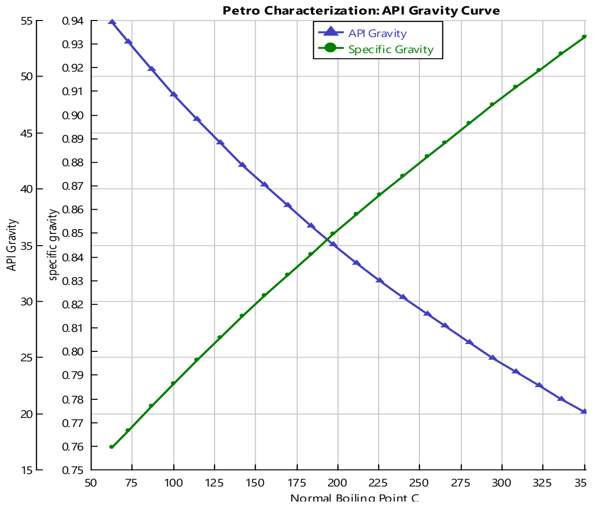


**Fig 9:** Specific Gravity & API versus NBP curve (RGF).

The relationship between API gravity and specific gravity as a function of NBP is seen in Fig. 9. The specific gravity has a range of 0.75 to 0.94, and its value rises as the temperature rises. It implies that the pseudo-component gets heavier at the curve's terminus.

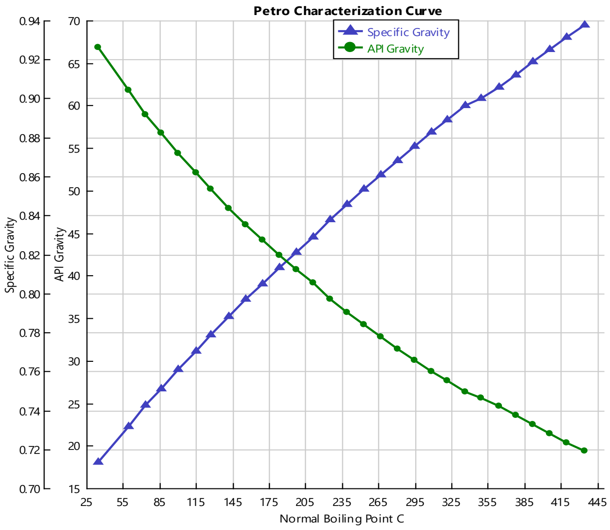


**Fig 10.** Specific gravity & API versus NBP curve (KTL).

The specific gravity ranges from 0.7 to 0.94 and the temperature from 32 to 434 degrees Celsius for the KTL condensate (Fig. 10). It unmistakably suggests that the KTL condensate, a lighter condensate sample, includes a higher proportion of distillate. In order to produce petroleum products, it is therefore a preferable idea to use it as feedstock in a refinery (Nelson, 2018).

## 4. Discussion

Compared to RGF condensate, KTL condensate has lower IBP and EP. As a result, this kind of condensate can swiftly create distillate products, but it also runs the risk of losing light products due to their low-temperature vaporization. However, since the price of residual fuel oil is based on its reference viscosity, the amount of residue is substantial for the heavier sample, which is for RGF condensate, which lowers product value. More distillate fuel oil is needed to lower viscosity to a reference level where the value of more viscous fuel oil is degraded as viscosity increases [13].

According to the average boiling point temperature, KTL feed requires a larger temperature range in order to completely distill the sample, which is a major worry from an economic perspective because the cost and distillation time will be higher for this type of lighter feed. The study implies that an appropriate blend of the lighter and heavier sample can be used to achieve all the goals of a refinery in light of the aforementioned findings. In this way, the heavier one will postpone the IBP point and the lighter one will reduce the amount of residue at the endpoint while also improving the quality of the final product. This paper outlines a straightforward, yet methodical and ordered, approach to determining petroleum assay. Two polynomial equations are proposed by the study for the two chosen samples. For this kind of sample, these equations can be used to generate pseudo components and determine the ultimate distillation point (100%). In addition to an economic validity analysis of the condensate as refinery feed-stocks, the study suggests improving the modeling of the condensate with the chromatographic composition of the inputs, the feed flow rate, and the fractional information of light ends.

## 5. Conclusion

While compositional analysis is typically used to define condensates, this study approached it a little differently than it would for crude oil. The work may be useful to oil refineries that are considering substituting condensate for crude oil in terms of evaluating feed-stocks, estimating economic value, and developing and simulating the refining process.

## 5. References


1. Riazi, M. R., & Daubert, T. E. (1987). Characterization parameters for petroleum fractions. Industrial & engineering chemistry research, 26(4), 755-759.
2. Chang, A. F., Pashikanti, K., & Liu, Y. A. (2013). Refinery engineering: Integrated process modeling and optimization. John Wiley & Sons.
3. ASTM Committee D-2 on Petroleum Products and Lubricants, Boldt, K., & Hall, B. R. (1977). Significance of tests for petroleum products. American Society for Testing and Materials.
4. Al-Assady, Q. M. A. A. (2009). Characterization of petroleum fractions. Iraqi journal of mechanical and material engineering, 9(2), 223-238.
5. Nelson, W. L. (2018). Petroleum refinery engineering. McGraw-Hill.

6. Mokhatab, S., & Economides, M. J. (2006). Process selection is critical to onshore LNG economics. World oil, 227(2), 95-99.
7. Rahman, M. (2013). Overview of natural gas condensate scenario in Bangladesh.
8. Ahmed, A. D., & Islam, M. S. International Journal of Petroleum and Geoscience Engineering.2015
9. Imam, B. (2005). Energy resources of Bangladesh. University grants commission of Bangladesh, Dhaka, 277.
10. Alarouj, M., Alomair, O., & Elsharkawy, A. (2020). Gas condensate reservoirs: Characterization and calculation of dew-point pressure. Petroleum Exploration and Development, 47(5), 1091-1102.
11. Standard Test Method for Distillation of Petroleum Products at Atmospheric Pressure 1. 100 Barr Harbor Drive, PO Box C7OO, West Conshohocken, PA 19428-2959, United States. : ASTM INTERNATIONAL. Designation: D 86 - 07.
12. Riazi, M. R. (2005). Characterization and properties of petroleum fractions (Vol. 50).
13. Fahim, M. A., Al-Sahhaf, T. A., & Elkilani, A. (2009). Fundamentals of petroleum refining. Elsevier.
14. Fritt-Rasmussen, J., Wegeberg, S., Gustavson, K., Sørheim, K. R., Daling, P. S., Jørgensen, K., ... & Holst-Andersen, J. P. (2018). Heavy Fuel Oil (HFO): A review of fate and behaviour of HFO spills in cold seawater, including biodegradation, environmental effects and oil spill response.

# Appendix

Component breakdown results of RGF

| Pseudo-component | Average NBP C | API gravity | Specific gravity | UOPK | Molecular weight | Critical temperature C | Critical pressure bar |
|---|---|---|---|---|---|---|---|
| PC2 | 63.01765 | 54.82247 | 0.759436 | 11.13743 | 19.66325 | 256.5475 | 41.95792 |
| PC3 | 72.59713 | 53.08554 | 0.766582 | 11.13743 | 20.73406 | 267.1957 | 40.18208 |
| PC4 | 86.49667 | 50.6763 | 0.77672 | 11.13743 | 22.3339 | 282.4942 | 37.81694 |
| PC5 | 100.3978 | 48.38785 | 0.786601 | 11.13743 | 23.98983 | 297.6229 | 35.67275 |
| PC6 | 114.4324 | 46.18981 | 0.796332 | 11.13743 | 25.93169 | 312.7312 | 33.70411 |
| PC7 | 128.4812 | 44.09336 | 0.805839 | 11.13743 | 27.6671 | 327.6957 | 31.90677 |
| PC8 | 142.2294 | 42.13431 | 0.814931 | 11.13743 | 29.4505 | 342.193 | 30.29594 |
| PC9 | 155.4988 | 40.32382 | 0.823518 | 11.13743 | 31.25357 | 356.0531 | 28.86457 |
| PC10 | 169.5383 | 38.48784 | 0.832412 | 11.13743 | 33.25073 | 370.5822 | 27.46772 |
| PC11 | 183.5686 | 36.72905 | 0.841115 | 11.13743 | 35.34034 | 384.968 | 26.17981 |
| PC12 | 197.5552 | 35.046 | 0.849615 | 11.13743 | 37.51852 | 399.1813 | 24.99213 |
| PC13 | 211.5846 | 33.4235 | 0.857974 | 11.13743 | 39.80033 | 413.3149 | 23.88755 |
| PC14 | 225.843 | 31.83744 | 0.866305 | 11.13743 | 42.22034 | 427.5574 | 22.84511 |
| PC15 | 239.5188 | 30.37195 | 0.874148 | 11.13743 | 44.6383 | 441.1068 | 21.91392 |
| PC16 | 254.5006 | 28.82518 | 0.882581 | 11.13743 | 47.39709 | 455.8299 | 20.96362 |
| PC17 | 264.9979 | 27.77588 | 0.888396 | 11.13743 | 49.39903 | 466.0731 | 20.33755 |
| PC18 | 280.2897 | 26.2952 | 0.896732 | 11.13743 | 52.41753 | 480.8914 | 19.47912 |
| PC19 | 294.4446 | 24.97242 | 0.904313 | 11.13743 | 55.31989 | 494.5019 | 18.73649 |
| PC20 | 308.5436 | 23.69788 | 0.911739 | 11.13743 | 58.31422 | 507.9605 | 18.04211 |
| PC21 | 322.5551 | 22.47142 | 0.919002 | 11.13743 | 61.39192 | 521.2417 | 17.39311 |
| PC22 | 336.3812 | 21.29832 | 0.926057 | 11.13743 | 64.5279 | 534.258 | 16.7896 |
| PC23 | 350.2924 | 20.15326 | 0.933049 | 11.13743 | 67.78151 | 547.268 | 16.21646 |
| PC24 | 360.8137 | 19.30964 | 0.938269 | 11.13743 | 70.30697 | 557.0514 | 15.8041 |

Component breakdown results of KTL

| Pseudo-component | Average NBP(°C) | API gravity | Specific gravity | UOPK | Molecular weight | Critical temperature(°C) | Critical pressure(bar) |
|---|---|---|---|---|---|---|---|
| PC33C | 32.65927 | 68.01967 | 0.709203 | 11.5559 | 14.2105 | 215.6721 | 44.55695 |
| PC59C | 58.87474 | 62.62394 | 0.728916 | 11.5559 | 16.60807 | 244.9968 | 39.25888 |
| PC73C | 73.40256 | 59.87251 | 0.739396 | 11.5559 | 18.0075 | 260.9556 | 36.75463 |
| PC87C | 86.51895 | 57.51732 | 0.748609 | 11.5559 | 19.31572 | 275.197 | 34.71202 |
| PC101C | 100.5042 | 55.12908 | 0.758188 | 11.5559 | 20.75904 | 290.2159 | 32.73266 |
| PC114C | 114.2107 | 52.90133 | 0.767348 | 11.5559 | 22.56952 | 304.7773 | 30.96709 |
| PC127C | 127.313 | 50.86793 | 0.775904 | 11.5559 | 23.98045 | 318.5568 | 29.4215 |
| PC141C | 140.9602 | 48.84217 | 0.78462 | 11.5559 | 25.52228 | 332.7703 | 27.94249 |
| PC156C | 155.8333 | 46.73341 | 0.793903 | 11.5559 | 27.28885 | 348.1059 | 26.46541 |
| PC170C | 169.7222 | 44.8504 | 0.80238 | 11.5559 | 29.02182 | 362.2873 | 25.19881 |
| PC184C | 183.6111 | 43.04452 | 0.810681 | 11.5559 | 30.8372 | 376.3394 | 24.02919 |
| PC198C | 197.5 | 41.31041 | 0.818816 | 11.5559 | 32.73681 | 390.2675 | 22.94651 |
| PC211C | 211.1135 | 39.67566 | 0.826636 | 11.5559 | 34.6821 | 403.8035 | 21.96123 |
| PC225C | 224.6604 | 38.10863 | 0.834274 | 11.5559 | 36.70124 | 417.1636 | 21.04817 |
| PC239C | 239.2133 | 36.48735 | 0.842325 | 11.5559 | 38.96449 | 431.3982 | 20.13509 |
| PC253C | 253.0154 | 35.00547 | 0.849822 | 11.5559 | 41.20231 | 444.7898 | 19.32793 |
| PC267C | 266.8942 | 33.56671 | 0.857229 | 11.5559 | 43.54334 | 458.153 | 18.56874 |
| PC281C | 280.8177 | 32.17202 | 0.864534 | 11.5559 | 45.98423 | 471.4589 | 17.85529 |
| PC295C | 294.7258 | 30.82477 | 0.871709 | 11.5559 | 48.51538 | 484.653 | 17.18669 |
| PC309C | 308.6362 | 29.52061 | 0.87877 | 11.5559 | 51.14035 | 497.7554 | 16.5583 |
| PC323C | 322.5161 | 28.26009 | 0.885703 | 11.5559 | 53.85287 | 510.7383 | 15.9682 |
| PC336C | 336.4074 | 27.03715 | 0.892535 | 11.5559 | 56.66091 | 523.6439 | 15.41156 |
| PC350C | 350.2677 | 25.85343 | 0.89925 | 11.5559 | 59.55538 | 536.4353 | 14.88736 |
| PC364C | 364.1665 | 24.70114 | 0.905883 | 11.5559 | 62.55035 | 549.1794 | 14.3906 |
| PC378C | 378.0559 | 23.58263 | 0.912417 | 11.5559 | 65.63488 | 561.834 | 13.92091 |
| PC392C | 391.9503 | 22.49509 | 0.91886 | 11.5559 | 68.81103 | 574.4147 | 13.47583 |
| PC406C | 405.8391 | 21.43785 | 0.925212 | 11.5559 | 72.07488 | 586.914 | 13.05392 |
| PC420C | 419.7324 | 20.40874 | 0.93148 | 11.5559 | 75.42705 | 599.3428 | 12.65324 |
| PC434C | 433.8788 | 19.38876 | 0.937777 | 11.5559 | 78.92782 | 611.9237 | 12.26568 |